ICOLD Symposium on Sustainable Development of Dams and River Basins, 24th - 27th February, 2021, New Delhi

VALIDATION OF WILLOWSTICK SURVEY TO MAP LEAKAGE PATHS OF DAM FOUNDATION

D.S. PARK
K-water Research Institute, Daejeon, Republic of Korea

M. L. JESSOP
Willowstick Technologies, Salt Lake City, USA

ABSTRACT

Identifying underground leakage paths is highly important for the safety reasons owing to seepage in hydraulic structures. The purpose of this case study paper is to research the applicability and validation of a recently developed magnetometric resistivity survey (MMR), which is called, "Willowstick survey" for mapping 3D subsurface leakage paths. This technology started to use in British dams and North America in applications for hydraulic structures having seepage-related issues, but is still not too common and there have been few papers to validate the technology. In this study, the newly developed magnetometric resistivity (MMR) geophysical survey method is applied to the testbed dam (YD dam) site to map 3D underground leakage paths reliably. Its applicability is verified by geotechnical investigation techniques such as borehole drilling and sampling, in-site Lugeon test, flow orientation and velocity test, and seismic tomography. A 3D electrical resistivity survey is performed independently and the results were compared and analyzed. The new magnetometric resistivity survey effectively detected geologic weaknesses (e.g., fault fracture) and potential leakage paths of the dam site foundation rocks. The results of this research are expected to be effective for dams, river banks, slopes, tunnels, and mines where leakage is an important issue.

1. INTRODUCTION

In the new design of structures or safety management of existing structures that are exposed to water, it is important to identify underground flow paths in terms of safety and efficient operation. In most geological engineering environments, in which water impermeability needs to be secured, it is essential to identify underground flow paths. Relevant examples are dams, river banks, and temporary coffer dams (ICOLD 2013).

Thus, one of the most important item for aging dam safety might be the impermeability of the core layer or foundation cut-off wall (FEMA 2015, ICOLD 1987, ICOLD 2000, Rice & Duncan 2009, U.S. Army Corps of Engineers 1993). If seepage rate measurement is not defined accurately, the signs of internal erosion and piping danger may not be visible thus presenting significant safety problems (ICOLD 1994, Park and Oh 2016). Obviously, a rapid increase of seepage rate means potential internal erosion of the dam embankment (Charles 2001, Fell et al. 2003, ICOLD 1995). Reduced or unmeasured seepage rate can also be a problem since it means that some of the drainage systems may be clogged or the seepage water is being dissipated elsewhere (Fell et al. 2015).

Therefore, the normal measurement of the seepage rate is very important for the proper management of a fill dam (ICOLD 2000). Most commonly, seepage water is measured by the flow rate calculation formula of the triangular weir in the seepage measuring room located at the center of the downstream toe of the dam (Lim et al. 2004). In order to effectively collect such seepage water, a seepage collection wall is usually installed on the downstream side of the dam in order to secure water that is trapped between the foundation rock and the retaining wall. If a normal seepage rate cannot be measured, it means that the seepage water is being dissipated somewhere along the foundation rock or the seepage collection wall.

A survey to find the flow path is an essential element for understanding the seepage vulnerability of the dam embankment or the foundation rock. However, there are few techniques to map the current underground flow paths in three-dimensions. Current industry practice mainly conducts 2D or 3D electrical resistivity surveys, with significant manpower and time to identify the leaks (Cho & Yeom 2007, Johansson & Dahlin 1996, Panthulu et al. 2001, Sjödahl et al. 2008).

In this study, a test site was established at the dam (YD dam) site where the reservoir water needed to be secured. The newly developed magnetometric resistivity survey (MMR), which is called, "Willowstick survey" (Kofoed et al. 2012),

was conducted in parallel with other types of geophysical exploration including a 3D electrical resistivity survey. Given that saturated or wet strata act as excellent subsurface electrical conductor, the Willowstick magnetometric resistivity survey energizes the seepage water with a signature electric current to track how seepage bypasses the wall. This electric current follows the water-saturated zones out of the reservoir through, beneath, and/or around the seepage collection wall. By identifying preferential electric current flow paths, the survey is expected to answer questions about where water from the reservoir bypasses the wall. This technology has been used in applications for hydraulic structures having seepage-related issues (Bruggemann & Francis 2014, Smith et al. 2009), but is still not too common. Therefore, a validation of the technology is attempted.

The characteristics and problems of the testbed site are introduced, and the procedures and outcomes of the Willowstick MMR survey and 3D electrical resistivity survey are described. After the MMR survey at YD dam site, we validated the proposed survey to find the leakage paths through a detailed geotechnical investigation. Thus, a site geotechnical investigation is addressed in an attempt to corroborate the survey results. Finally, the results are analyzed and discussed. Some useful findings are presented.

2. THEORY

The detection of channels of preferential water flow is a common problem in engineering geology or hydrogeology. Although the problem is challenging, a promising fact is that groundwater is a predominate factor increasing the electrical conductivity of subsurface materials in most situations. It has been established that most earthen materials are fundamentally electrical insulators with conductivities ranging between 10^{-12} and 10^{-17} mho/m, yet in-situ measurements of electrical conductivities range from 10^{-1} to 10^{-8} mho/m, in other words, many orders of magnitude higher due to the presence of groundwater (Purvance & Andricevic 2000). This fact has led to widespread use of electrical and magnetometric resistivity methods for groundwater investigation, and today these methods are appropriately recognized as being among the most powerful tools for hydrogeophysical investigation at the field scale (Yaramanci et al. 2005).

The Willowstick MMR method is a rapid and effective way to utilize highly sensitive magnetic technology to detect subsurface channels of preferential water flow (Kofoed et al. 2013). Magnetic measurements are made in free space, without requiring galvanic contact with the ground. The survey setup involves identification of strategic energizing points to energize groundwater directly, and it is most effective when electrodes are placed in a manner to create current flow along an elongated conductive target, or along the anticipated direction of hydrologic flow. Once electrodes and circuit wire are positioned, a low-frequency electric circuit is established to create a subsurface electric current flow (non-inductive), and an associated magnetic field (also non-inductive) is produced. This magnetostatic response contains information on the subsurface electrical resistivity structure, reflecting among other things, variations in lithology, water content, and water salinity (Yaramanci et al. 2005).

3. APPLICATION TO DAM SITE

3.1 Testbed dam

The YD dam is a CFRD (Concrete Faced Rockfill Dam) with a height of 70 m and a length of 498 m constructed in 1999 (KNCOLD 2004) (Figs. 1-2). The YD dam is equipped with seepage rate measurement room on the downstream part for the safety management of the dam, and a retaining wall was installed on the downstream side of the measurement room for collecting seepage water passing through the dam and foundation rock (Figs. 1-2).

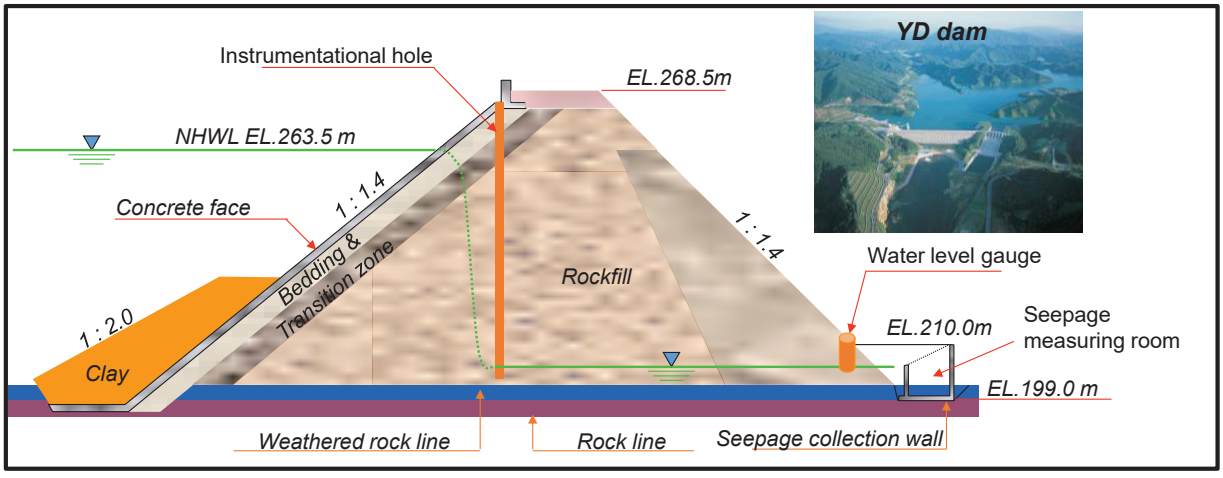

Figure 1 : Typical cross-section of YD dam

Figure 2 : YD testbed site map

However, it is impossible to quantitatively measure the amount of seepage until the measurable water level reaches the appropriate level within the seepage rate measurement room as shown in Figure 3. During the dam operation, it has been necessary to activate the seepage quantity measurement, but it was difficult to establish proper measures due to the unknown cause of leakage and ambiguity of the leakage paths (K-water Research Institute 2016).

The difficulty of measuring the seepage quantity was expected to be the water leakage occurring either, (1) through the junction of the retaining wall and the foundation or, (2) through each joint of the retaining wall, and/or (3) through the jointed foundation rock mass. The construction history record demonstrated that there was no grout curtain underneath the retaining wall.

In order to identify, map and model any preferential flow paths through, beneath and/or around the seepage collection wall, a newly developed (Willowstick) MMR survey and the existing 3D electrical resistivity survey were performed on the YD dam site. Later, the outcome was utilized to validate the applicability of the survey through the geotechnical investigation.

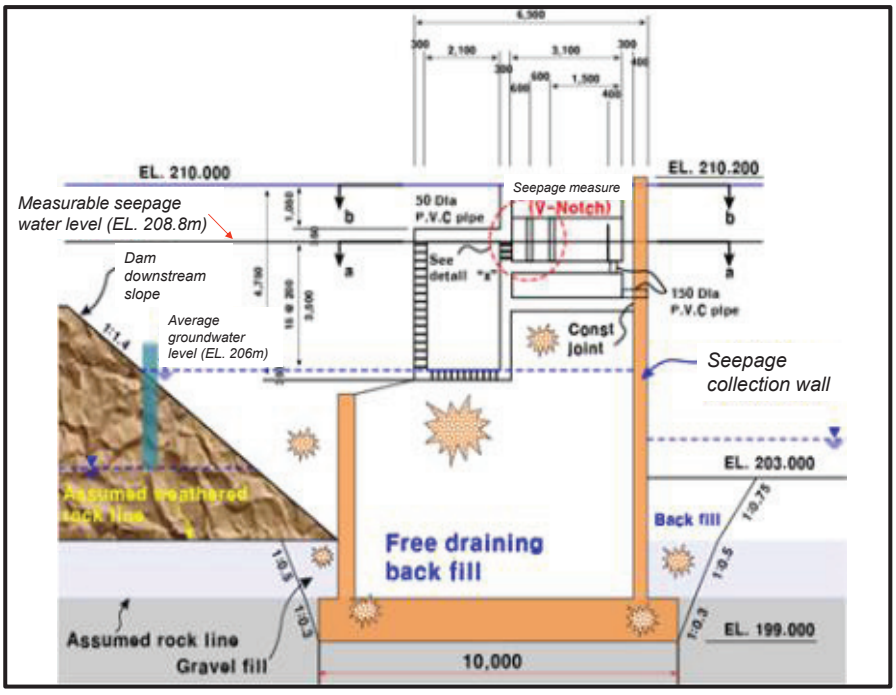

Figure 3 : A cross-section of seepage measuring room and the status of seepage water table

3.2 Willowstick survey application

The Willowstick MMR survey entailed mapping cultural features pertinent to the investigation, laying out circuit wire and placing electrodes strategically thus energizing the subsurface study area, and measuring and recording the magnetic field on dam's downstream face and around the seepage collection wall (Kofoed et al. 2006). The fieldwork took approximately 2-3 days to complete. Figure 4 presents a cross-sectional schematic (not necessarily to scale) of the electrode configuration used for the investigation.

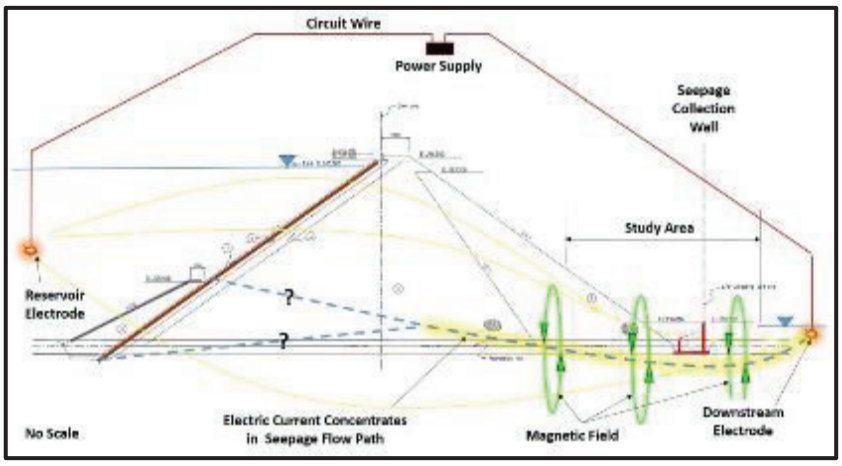

Figure 4 : Typical horizontal dipole configuration

A horizontal dipole was established with an up-gradient electrode in the reservoir and a down-gradient electrode in the receiving waters located downstream of the seepage collection wall. The circuit was energized with a specific AC signature frequency at 380 Hz. As electric current chose its path between the paired electrodes, its signature magnetic field was measured from the ground surface (Montgomery & Kofoed 2008). The magnetic field was measured and used to identify the distribution of electric current flow through, beneath and around the seepage collection wall. By identifying the electrically conductive flow paths between the electrodes, it becomes clear where seepage potentially exists through, beneath and/or around the wall.

Figure 5 presents the electrode configuration and survey layout for the investigation, as well as site features pertinent to the investigation. As shown, the study area targets the downstream face and seepage collection wall. Numerous small red symbols denote measurement stations, which were established on a 10 m by 10 m grid. Many measurement stations were occupied repeatedly for quality control purposes. The circuit continuity, magnetic field strength, and signal-to-noise ratios were strong throughout the survey area. The position and elevation of each measurement station was recorded as part of the fieldwork, which is critical to quality control measures, data processing, modeling and interpretation.

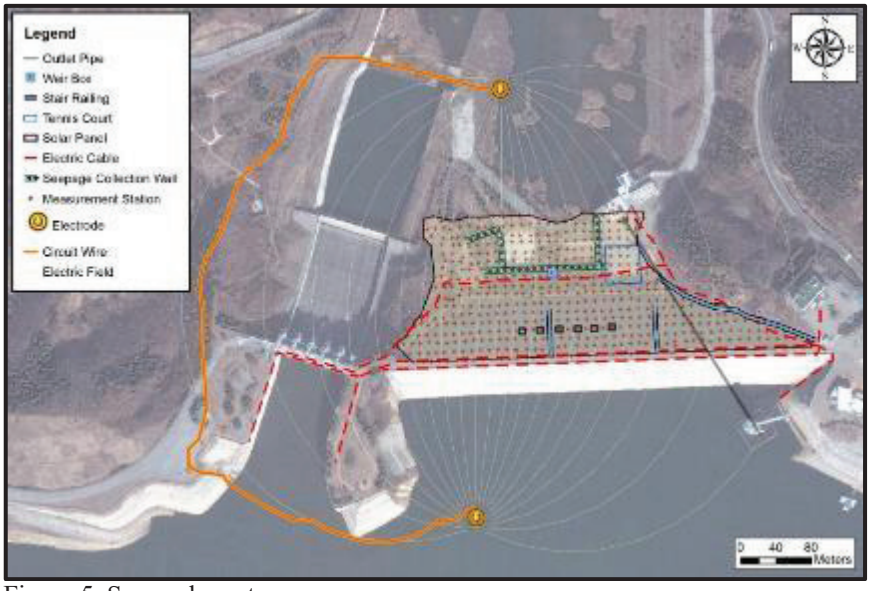

Figure 5 : Survey layout

After collecting the magnetic field data, the data was reduced and filtered. In some locations, conductive culture was present. Conductive culture is any man-made electrically conductive feature such as steel fence lines, electrical grounding systems, metallic pipelines, power cables, metal railings and/or other long continuous conductors. Conductive culture reduces the total amount of electric current flowing through the subsurface, and it can limit the ability to interpret nearby

seepage flow paths by producing higher amplitude anomalies that can overshadow anomalies from the subsurface. Negative effects of conductive culture can be mitigated by filtering. For this project, the known conductive culture was taken into account during the interpretation of the data.

Figure 6 presents the magnetic field observed when the study area was energized with the signature electric current. The "observed" magnetic field data is difficult to interpret directly, and the subsurface current flow is mixed with interference from conductive culture in many parts of the study area. To better interpret the data, it was filtered and compared to the expected magnetic field for a homogeneous earth case—or compared to what it would be if the subsurface were electrically homogeneous—which can be calculated by proper application of known geophysical principles (e.g., Edwards et. al. 1991). The comparison of measured data to that expected from a homogeneous earth is useful. For example, the electric current density may be 60% stronger at a particular location than it would be in the "homogeneous-earth" case. The comparison causes true heterogeneity (due to subsurface differences) to stand out or become more visible. Extreme care was taken in all survey configurations so that heterogeneity due to proximity, geometric relationship with electrodes, circuit wire, and topography are prevented from influencing the results of the survey. Fundamentally, the technology detects the preferred connective and conductive pathways between two selected points, and in order to do so, the signal emerging from preferred paths of electric current flow must be distinguishable from the diffuse or "background" flow pattern—which is always present and is often the dominant part of the signal. The background flow pattern can also be expected with proper application of the laws of physics, enabling subtler preferential electric current flow paths to be detected than would otherwise be possible.

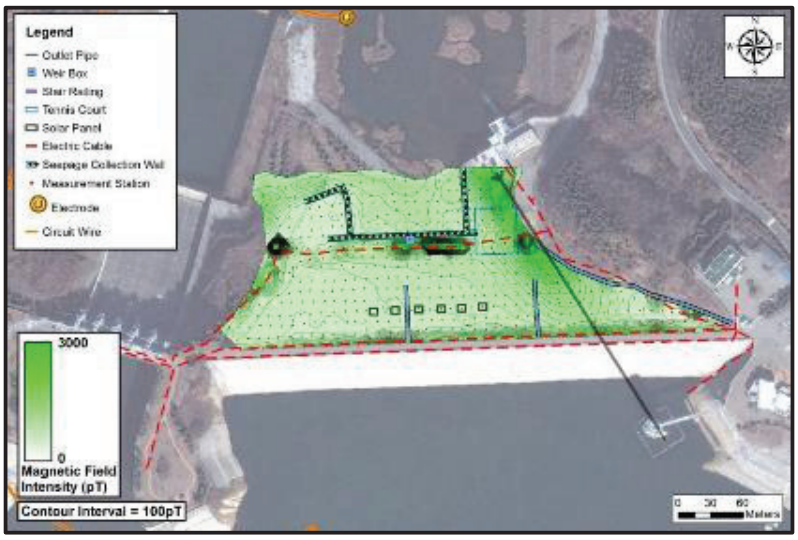

Figure 6 : Observed magnetic field contour map

Figure 7 shows the expected magnetic field in the case of an electrically homogeneous subsurface. The expected characteristics take into account the 3D layout and terrain in addition to electrode and wire position. The expected result becomes important to compare and correct the measured magnetic field so that the concentration of electric current due to heterogeneity (variations in conductivity, such as that caused by seepage conditions) to stand out, which facilitates interpretation and modeling.

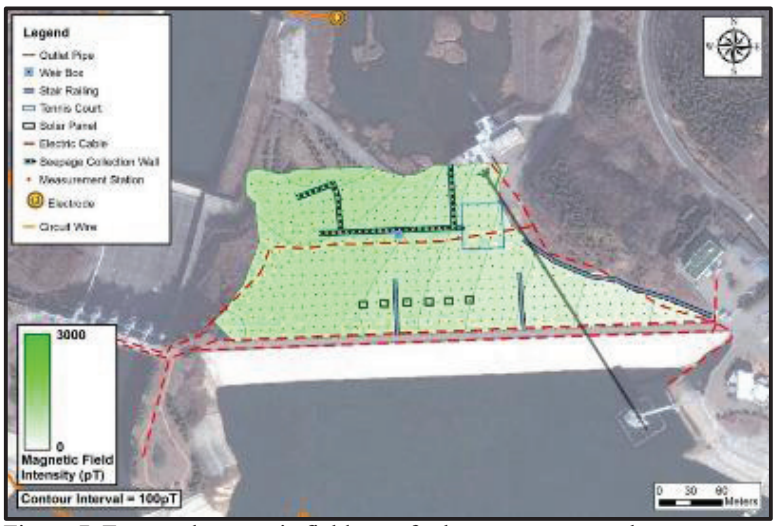

Figure 7 : Expected magnetic field map for homogeneous earth

By comparing the observed magnetic field data with the expected magnetic field data, a ratio response map is created which removes electric current bias from the data set and shows areas of anomalous electric current flow—greater or lesser than expected (Figure 8). In Figure 8, the white shaded contours (where the ratio is approximately 1:1) show where the magnetic field intensity is equivalent to that expected by the homogeneous model. Areas shaded purple indicate magnetic field is less than expected, and areas shaded green indicate magnetic field is greater than expected.

A significant amount of electric current flows onto near-surface conductive culture, most notable along the outlet pipe and the electric cable at the toe of the dam. Conductive culture is also observed along the crest, stair railing and electric cable located near the right abutment miter joint. Anomalies from conductive culture are often present and must be mitigated to precisely interpret the preferential flow paths of the magnetic signal.

Magnetic field measurements influenced by near-surface conductive culture were identified and filtered by three criteria that were applied to the data set: Normalized gradient filter, distance filter, and point-specific professional judgment (Kofoed et al. 2012). In addition to filtering, in some cases the effects of conductive culture on the magnetic field can be modeled accurately enough to be removed from the data. This process was used to model and predict the strong current flow along the outlet pipe and effectively remove it. This allowed for a much better interpretation near the outlet pipe.

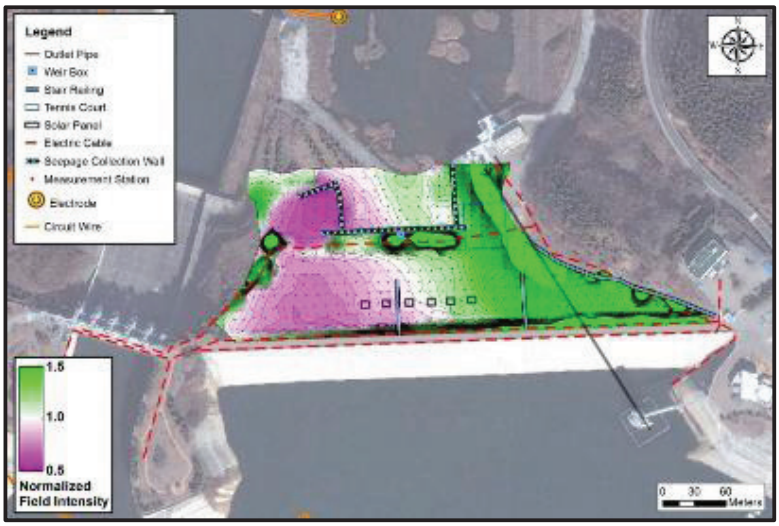

Figure 8 : Ratio response map

Figure 9 presents a revised ratio response map after filtering and modeling out the strong effect of the outlet pipe. Even though an extensive effort was made to remove all influence of conductive culture, some of the interference could not be removed. Nevertheless, the filtered map is much improved.

Interpretive markings (yellow lines and arrows) have been added to the figure to help explain the preferential paths of electric current that are clearly evident in this "footprint" map. As electric current flows out from the reservoir electrode through the dam, it tends to concentrate beneath the right half of the dam and move toward the southeast corner of the seepage collection wall. About 30 meters upstream of the wall the seepage bifurcates. Much of the seepage eventually flows beneath the south leg of the wall while an apparently lesser portion flows northward and beneath the wall's northeast corner.

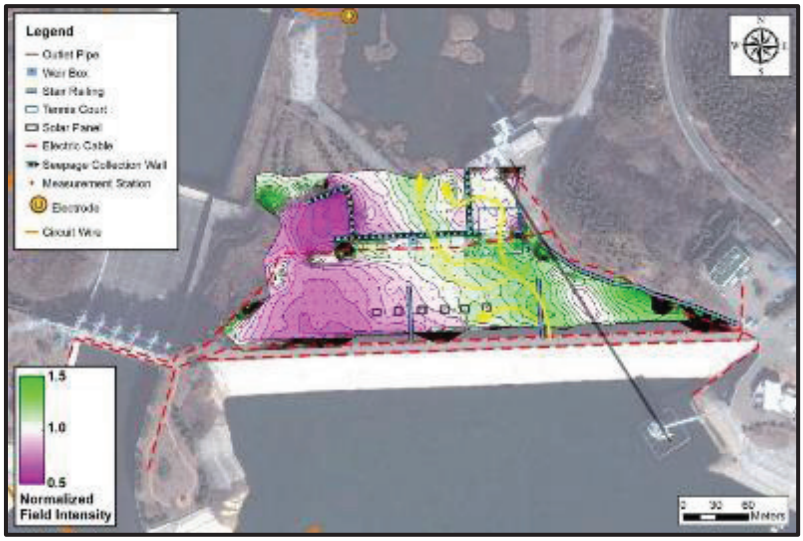

Figure 9 : Corrected and filtered ratio response map

Since the magnetic field is only measured from the ground surface (above a preferential flow path) and not below or beside the path, the most effective way to determine the depth of the preferential electric current flow is to model it using data collected during the investigation. The data is processed by an inversion algorithm designed to predict the distribution of electric current flow in three-dimensional space within the subsurface study area. The inversion result is referred to as an Electric Current Distribution (ECD) model. Figure 10 presents an example of slices through the ECD model. In the model, the dark green shading identifies areas where electric current density is more concentrated than expected. The dark purple shading identifies areas where electric current is less concentrated.

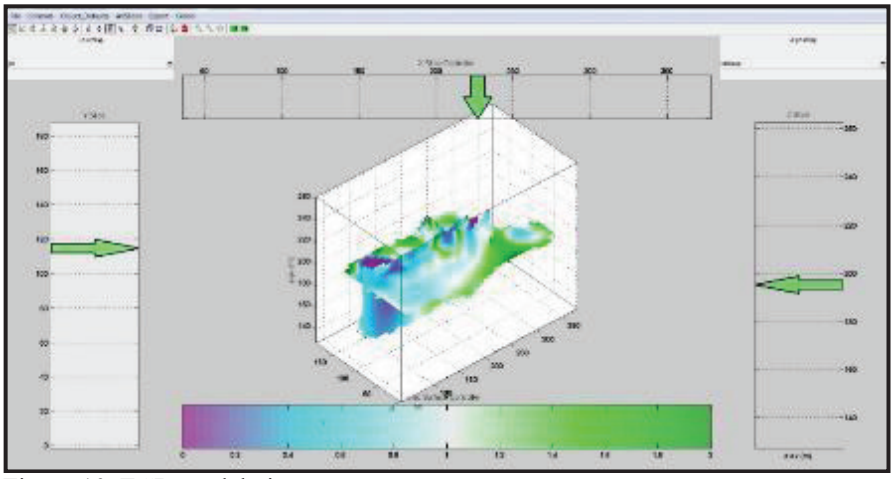

Figure 10 : ECD model viewer

In addition to the ECD model, a 3D site model was created to show pertinent site features in relation to ECD model slices. Figure 11 presents a view of the 3D site model. To facilitate data analysis and interpretation, ECD model slices are either presented in map view or are embedded in the 3D site model.

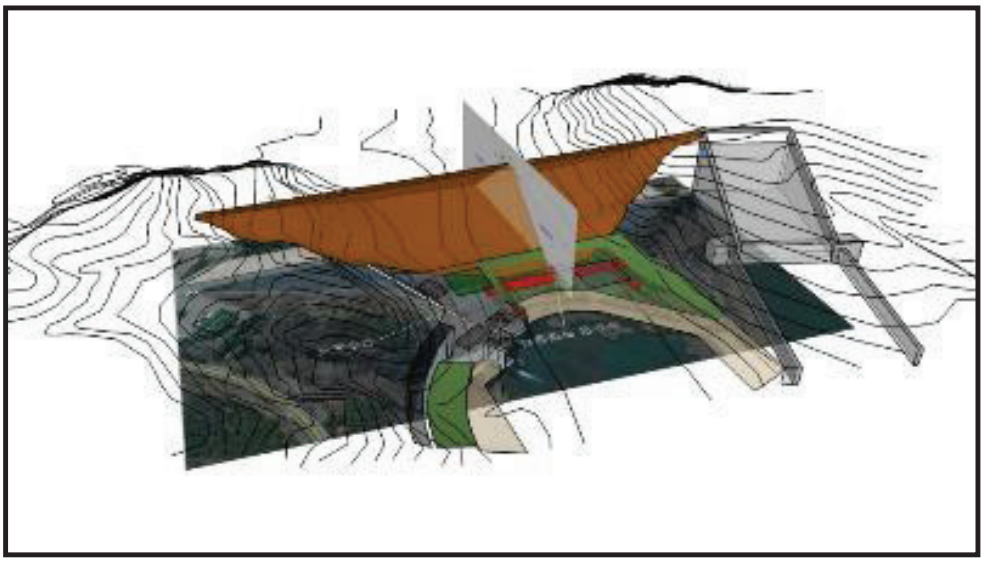

Figure 11 : 3D site model (looking upstream)

3.3 3D electrical resistivity survey

A three-dimensional electrical resistivity survey (Samouëlian et al. 2005, Wilkinson et al. 2010) was carried out mainly on the downstream area at the YD dam site, for comparative research purposes. A total of 12 lines were arranged for the survey. Figure 12 shows the 3D electrical resistivity survey location map. The survey method encompassed to arrange measuring points using tape measure and GPS, install the electrode and cable, check the ground resistance and measure the data. In order to improve the quality of the data, dipole-dipole method and modified pole-pole method were used. Some lines (Line 3, Line 4, Cross 3, and Cross 4) had a yard section with cement pavement, and exploration was carried out by drilling cement. The total survey line length was 1,240 m. The equipment used in the 3D electrical resistivity survey is SuperSting R8 / IPTM (AGI, USA). The software used for the inverse 3D resistivity analysis was DC3DPRO developed by the Korea Institute of Geoscience and Mineral Resources. This software can provide improved underground images by setting the information of the 3D coordinates (X, Y, Z) and the actual terrain of the existing 2D resistivity survey data.

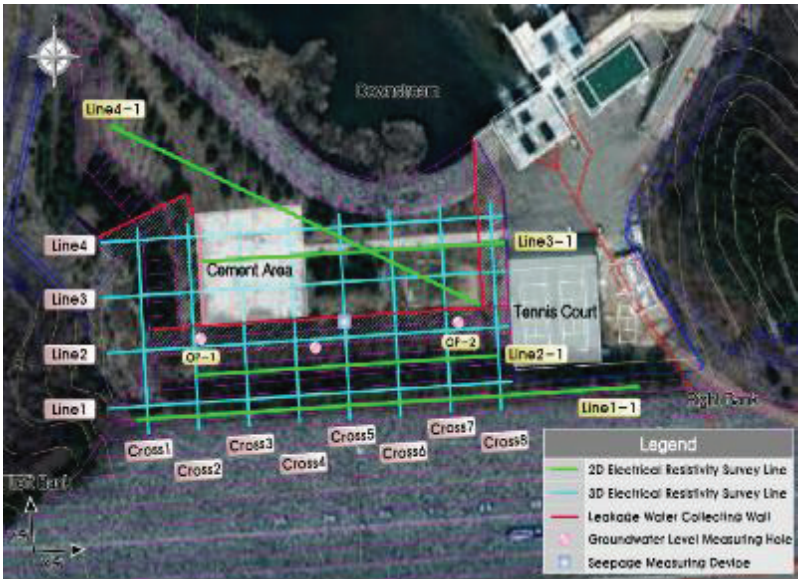

Figure 12 : Layout of 3D electrical resistivity scheme

4. RESULT

4.1 Willowstick survey result

The survey identified two seep paths, a primary path and a possible secondary path. These paths appear to pass beneath the seepage collection wall.

Figure 13 shows a horizontal slice of the electric current distribution (ECD) model. The slice is taken beneath the bottom of the seepage collection wall which is at an approximate elevation of 199 m. The ECD model colors are calibrated so that white shading indicates areas in which the electric current density is equivalent to the expected amount for an electrically homogeneous subsurface model. Areas shaded blue-to-purple indicated the electric current density is less than expected, and areas shaded green indicate the electric current density is greater than expected.

The highlighted yellow path identifies a primary seep path beneath the seepage collection wall. The dark blue line with nodes labeled A through I identifies a weakness or geologic feature (e.g., a small fracture or paleo channel beneath the original river channel) where seepage concentrates and flows beneath the wall. The solid orange line with nodes labeled 1 and 2 identifies an apparent secondary seep path beneath the wall. The noted seep paths have been ranked primary and secondary based on the intensity of the magnetic field and overall evidence of the path, suggesting that more water bypasses the seepage collection wall along the primary path than along the secondary path.

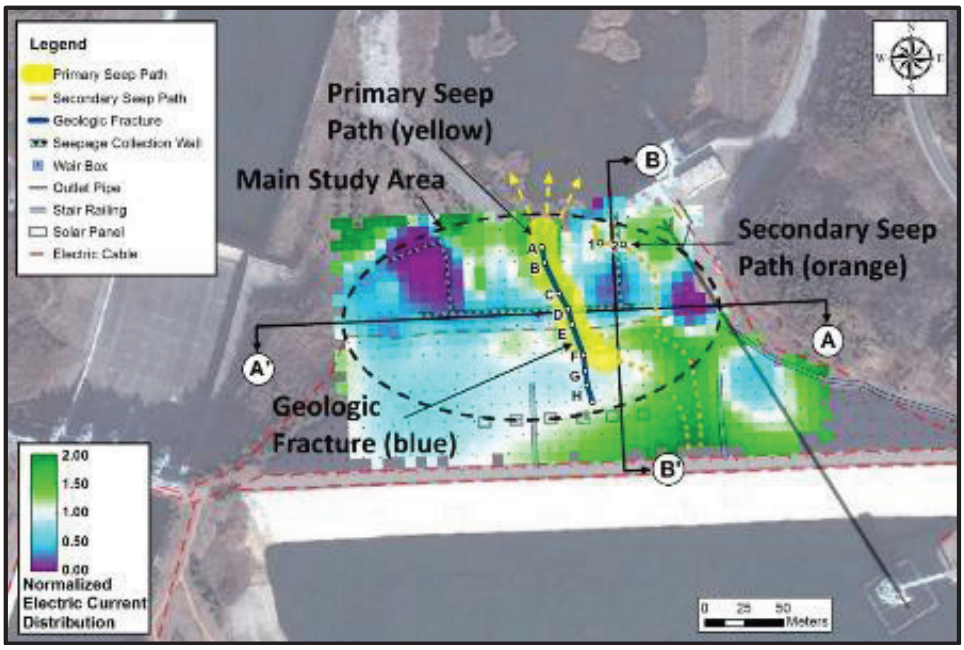

Figure 13 : Summary of the MMR survey

To further describe seepage beneath the wall, Figs. 14 and 15 present Sections A-A′ and B-B′. Cross-section A-A′ is taken along the south leg of the seepage collection wall. The seepage depth is estimated to be at an elevation of approximately 192 m. Cross-section B-B′ is taken along the east leg of the seepage collection wall, where the secondary seep path appears beneath the seepage collection wall at elevation 195 m, approximately. No other seep paths were identified through, beneath or around the seepage collection wall.

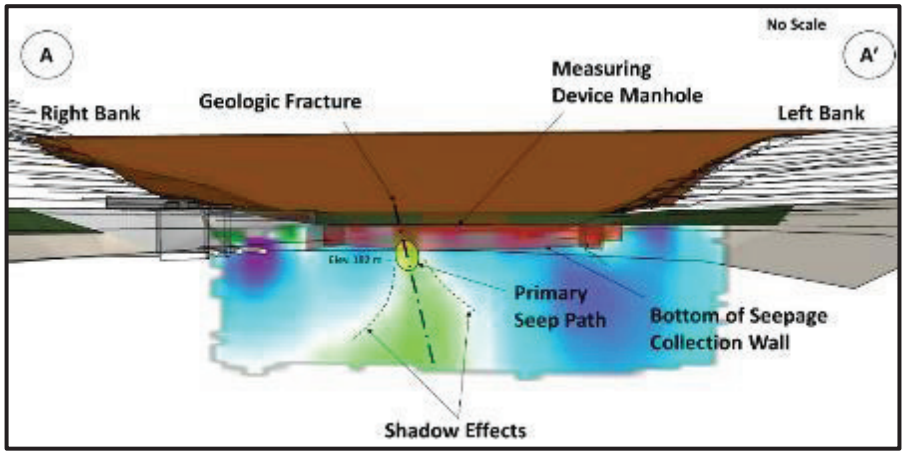

Figure 14 : Section A-A′ (looking upstream)

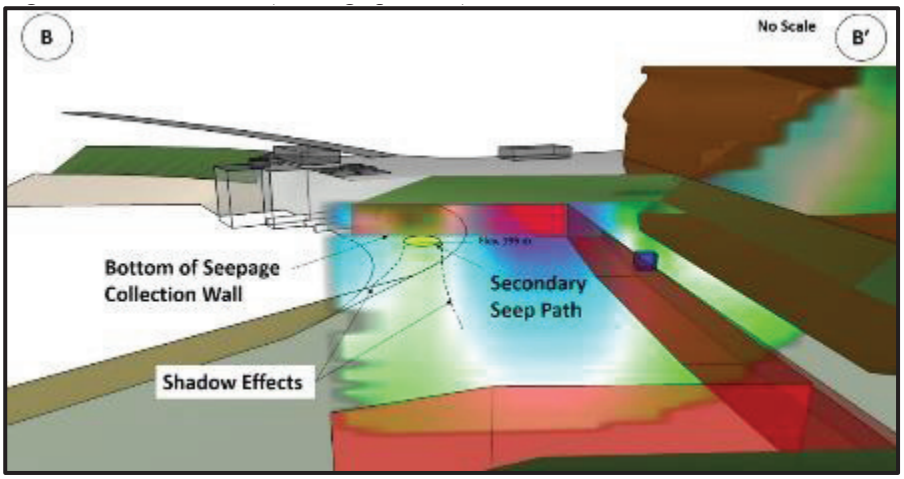

Figure 15 : Section B-B′ (looking east)

The ECD model slices were used to carefully analyze the distribution of electric current flow in three-dimensional space to best locate preferential flow paths. Coordinates of the center of the paths were provided.

To understand the accuracy of the ECD model and the preferential flow path identified by model analysis, a few considerations must be noted. The maximum horizontal error in the position of preferential flow is ¼ to ½ the spacing between data stations. For this investigation, a 10 m grid spacing was used. Therefore, the horizontal error would be within 2.5 to 5 m, maximum. The ECD model provides an estimation of depth, but the accuracy of depth estimation depends on some factors that should be more carefully considered. The ability to estimate depth accurately is primarily dependent upon the degree of channelization or "focusing" of electric current. For example, experience with modeling shows that the depth accuracy can be as good as 5-10% (of the depth in question) where a high degree of channelization of electric current exists along well-defined flow paths. On the other hand, if electric current is more evenly dispersed without any "channeling", then the preferential path is more difficult to determine in such a precise manner. In this investigation, the noted flow paths manifest as fairly strong heterogeneity (more so along the primary flow path). Therefore, the depth accuracy is expected to be fairly good (~15 to 25%). It should also be noted that interference from conductive culture can also adversely affect the estimation of depth, especially if the location of conductive culture is not known.

Although the survey can identify the center of the flow path within the tolerances described, it does not specifically identify the edges of the flow path. While, the breadth of the seep path can be approximated, the extent of seepage flow paths should be verified by other field methods. It is recommended that the results of the investigation be compared with all known site information to further characterize, monitor and possibly remediate conditions regarding seepage flow beneath the seepage collection wall.

4.2 3D electrical resistivity survey result

Figure 16 shows the results of three-dimensional resistivity inversion (X in dam axis direction, Y in stream direction, and Z in vertical direction). The section in the X-Y direction is the plane in the elevation, the section in the X-Z direction is the plane in the dam axis direction, and the section in the Y-Z direction is the plane in the stream direction. The low resistivity zone (in blue color) is beginning to form at the bottom of the seepage collection wall in the EL.206 m section, which is very similar to the groundwater level observed at the downstream measurement holes (OP-1 and OP-2 as shown in Figure 12). The average groundwater level of OP-1 is 206.2 m, and that of OP-2 is 206.4 m. In the result section of EL.204 m, low resistivity band is located in the seepage collection wall section. In the result section from EL.199 m to EL.185 m, the low resistivity zone is extended to the whole seepage collection wall section.

Figure 17 is the result of the XZ section parallel to the dam axis. The result section at Y = 33 m is the section where the groundwater level measurement holes (OP-1, OP-2) are located. The lower part of EL.206 m which is the average groundwater level, shows low resistivity band as a whole. On the other hand, the result of Y = 60 m, which is more downstream than that of Y = 33 m, shows that the low resistivity band is considerably reduced.

Figure 18 is the result of cross-section in the Y-Z direction orthogonal to the dam axis. All the results show that the low resistivity band is developed deep into the bottom of the seepage collection wall.

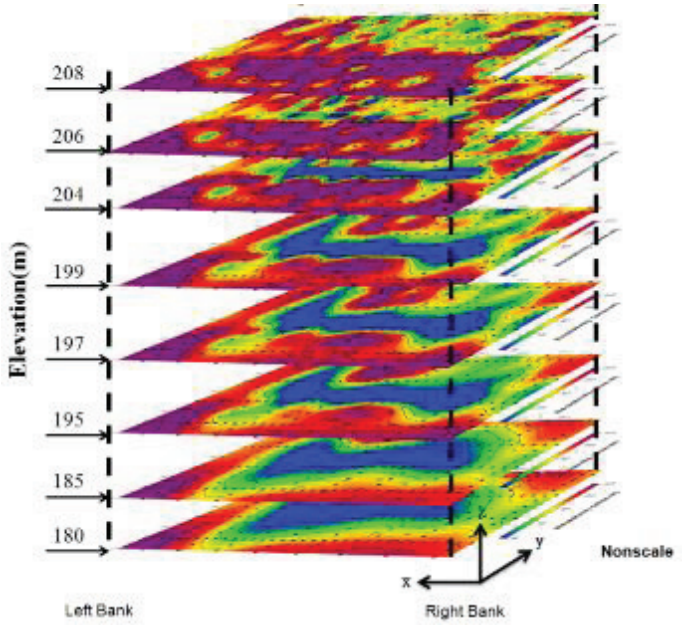

Figure 16 : Stacked slice images along X-Y direction

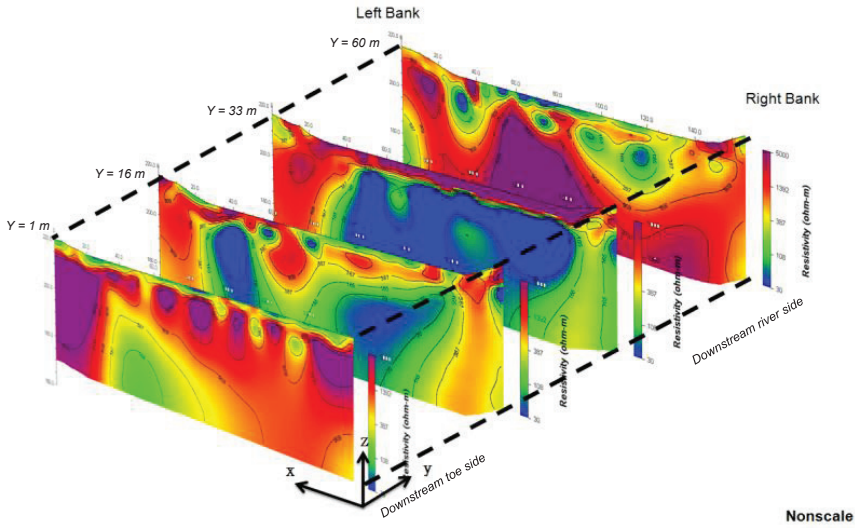

Figure 17 : Stacked slice images along X-Z direction

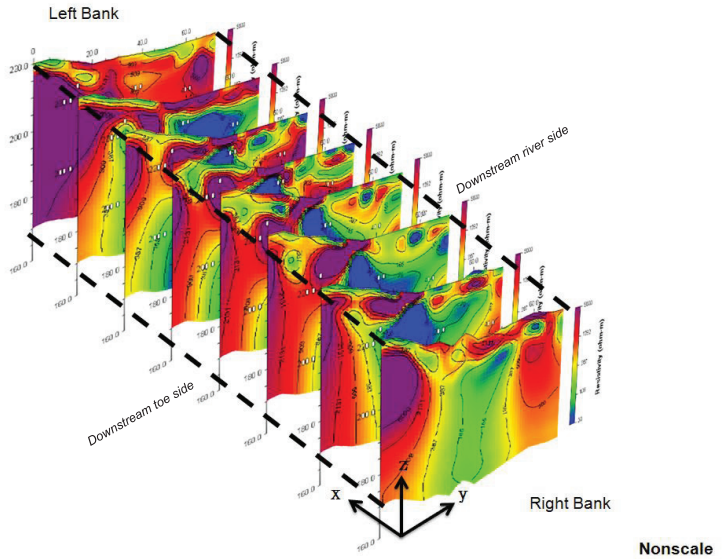

Figure 18 : Stacked slice images along Y-Z direction

4.3 Comparison

In Figure 19, the results of the Willowstick MMR survey and the 3D electrical resistivity survey were compared. The results of the electrical resistivity survey show that the bottom of the seepage collection wall has low resistivity as a whole. And it is confirmed that the primary leakage path estimated by the MMR survey is located within the low resistivity zone.

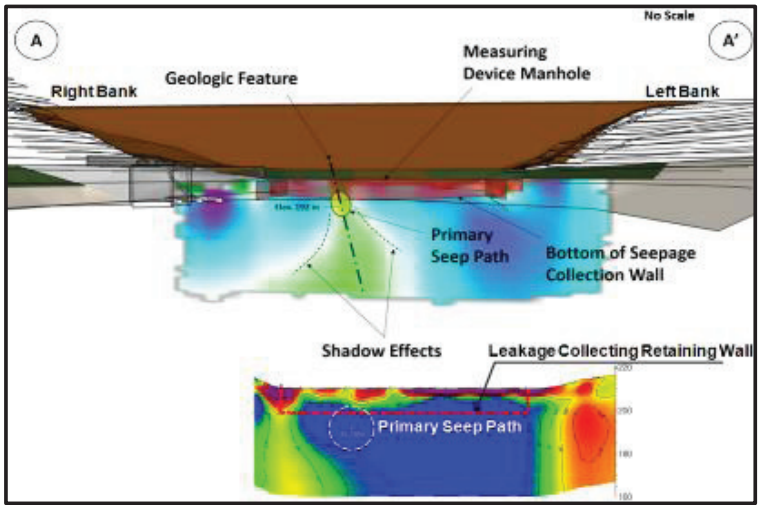

Figure 19 : Comparison of both results for A-A' vertical section on seepage collection wall

In Figure 20, the results of the MMR survey show that the secondary leakage path occurs at EL.195 m in the right side of the wall. However, in the result of the electrical resistivity survey, there is no observed low resistivity area in the right side of the wall. The points that are estimated as the secondary seepage path from MMR survey shows rather high resistivity values.

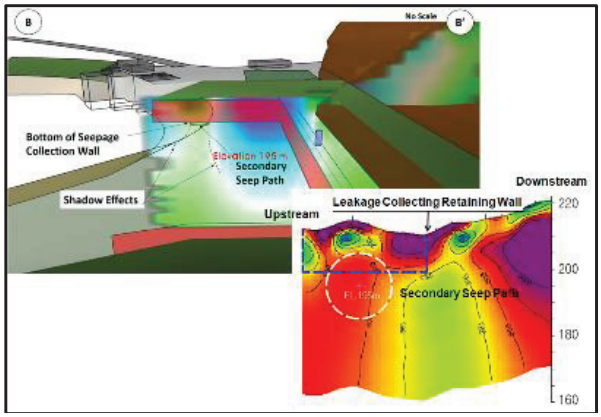

Figure 20 : Comparison of both results for B-B' vertical section on seepage collection wall

In Figure 21, we compared the low resistivity area of the resistivity survey at EL. 199m (in blue) and the leakage path location of the MMR survey at EL.195m (in yellow). The MMR survey estimates that the main leakage occurs on the right side of the seepage measuring room. On the other hand, resistivity survey does not clearly reveal any preferential leakage paths, rather, shows overall low resistivity area along the seepage collection wall.

The main leakage path obtained from the two survey results are somewhat different, but they all agree in terms of leakage occurring underneath the seepage collection wall base. With resistivity data, groundwater level was effectively delineated, but it did not effectively provide the underground flow paths. From the comparison, the MMR survey is a technique to find a selective flow paths underground, while 3-Dimensional electrical resistivity works well to find the groundwater level.

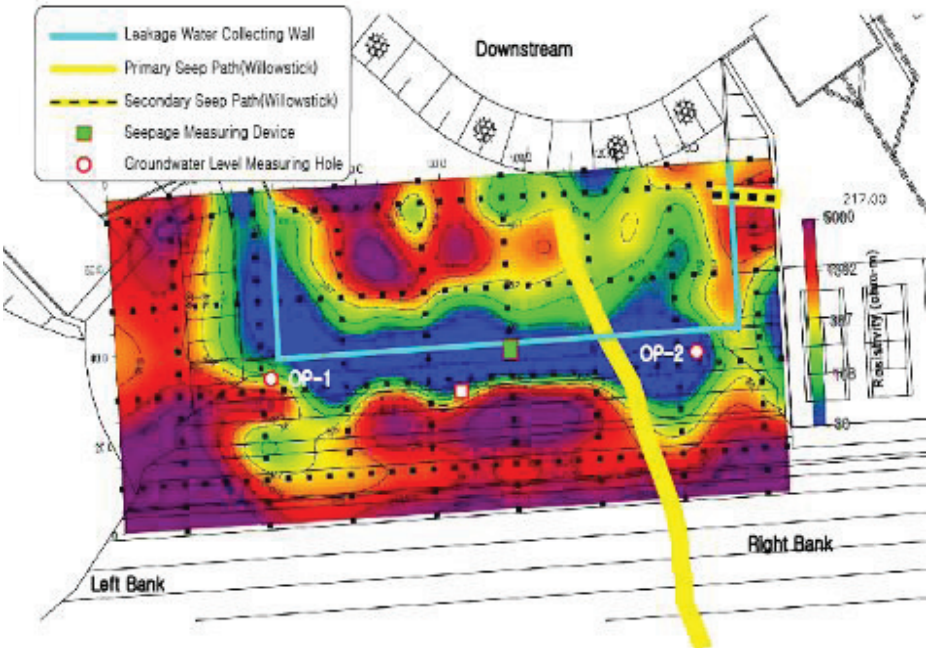

Figure 21 : Comparison of (1) primary seep path by Willowstick MMR survey results and (2) low resistivity anomaly around seepage collection wall by electrical resistivity on the sectional plane (EL. 199m)

5. VALIDATION

5.1 Geotechnical investigation

Geotechnical investigation including targeted borehole drilling and sampling, in-situ Lugeon test, flow orientation and velocity test, and seismic tomography was conducted to validate the MMR survey results for the YD dam site. This data will also be used as the basis for determining the optimum remediation grouting work to normalize YD dam seepage rate measurement in the future. Table 1 and Figure 22 show the geotechnical investigation scheme conducted.

Table 1 : Geotechnical site investigation scheme and quantity

Borehole	depth (GL-m)	SPT	Lugeon test	Flow orientation & velocity	Groundwater level	Seismic tomography
BH-1	31.0	3		2	1	
BH-2	34.0	5	2	2	1	
BH-3	25.0	4	1	1	1	
BH-4	15.0	3				
BH-5	11.3	4			1	
BH-6	34.0	3				1
BH-7	34.0	3				

The borehole drilling was carried out in a NX-sized core barrel using a rotary wash type drilling machine and the depth of drilling reached to 2 ~ 3 m to soft rock under the expected fracture zone. To prevent collapse of the borehole wall during drilling, the casing was inserted to the depth where the wall did not collapse. A perforated PVC pipe was buried in the ground for groundwater level and flow characteristic measurement. A standard penetration test was carried out during the drilling process. The rock core was sampled using a D-3 core barrel. Figure 23 shows the sequence of borehole drilling.

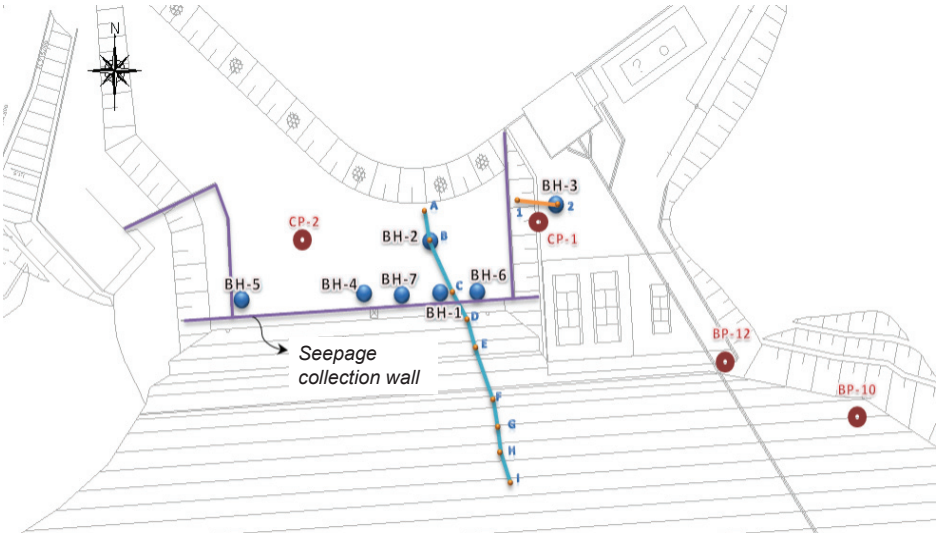

Figure 22 : Location map of borehole drilling

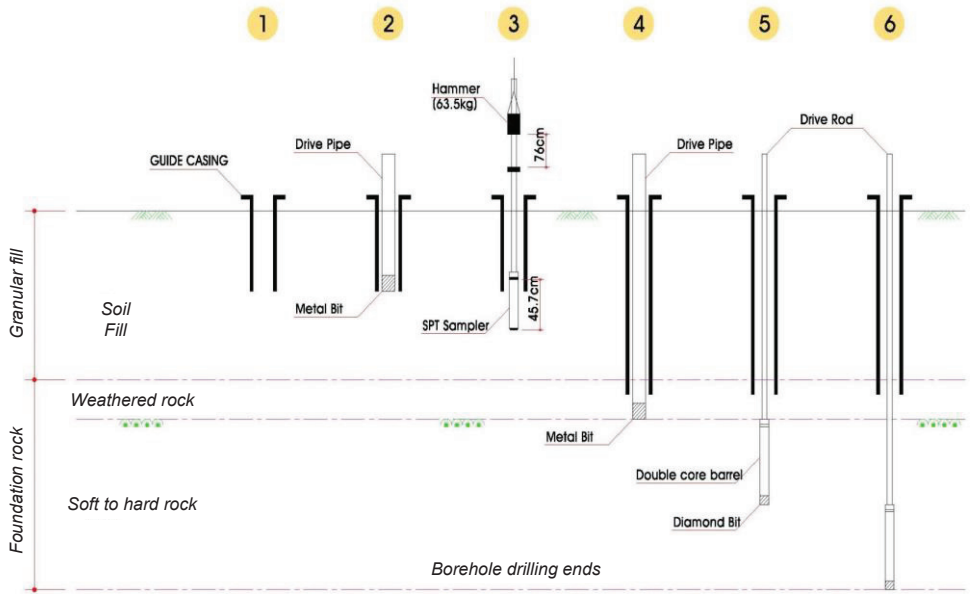

1. *Installation of guide casing (for soil layer)*
2. *Pushing to the Standard Penetration Test (SPT) position*
3. *SPT*
4. *Installation of the guide casing up to the section where the wall can be maintained and pushing to the top of rock*
5. *Coring with D3 core barrel*
6. *Borehole drilling to the targeted depth*

Figure 23 : Borehole drilling flowchart

Lugeon test was performed to confirm the permeability of the rock. The pressure stage is divided into 2 to 10 kgf/cm^2. After gradual increase of the pressure, pressure is reduced to 8, 6, 4 and 2 kgf/cm^2, respectively.

Groundwater flow orientation and velocity measurement was partially performed to find the leakage flow direction and velocity at certain depths. It is typically affected by a rock discontinuity distribution. The test was carried out five times in the BH-1 and BH-2, which was expected as the main leakage path of the MMR survey, and in the BH-3, which was expected as the secondary leakage path. The location of the fracture zone, which is considered to be more permeable, was selected with reference to the drilling log. After the sensor was inserted, the heat pulse was applied and the temperature was maintained for 10 to 15 minutes, and the heat pulse was measured for about 1 hour. In order to confirm the accurate water level, automatic observation of groundwater level was performed using the Mini-Diver.

The seismic tomography was carried out in order to understand the inter-behavioral structure of two neighboring boreholes (Nolet, 1987). Two boreholes (BH-6, BH-7) were used for logging (Figure 24). BH-7 was used as the transmitter and BH-6 was used as the receiver.

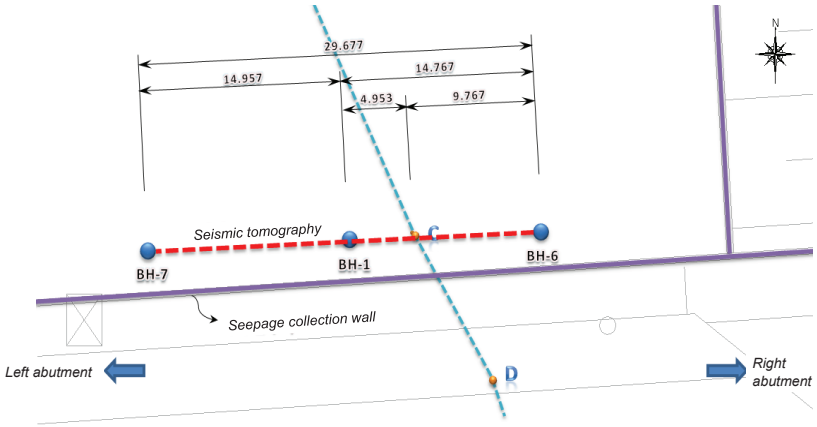

Figure 24 : Seismic tomography location map

As a result of borehole drilling, the strata were distributed as upper granular fill layer, dental concrete, and weathered and soft bedrock (Table 2). Dental concrete was found to be 0.5 to 1.7 m thick at BH-1 and BH-6 boreholes. In the BH-6, the stratum of dental concrete is considered as a ground improvement measure to replace a fault fracture band according to construction history documentation.

The drilling log of BH-1 and BH-2, which is expected as a primary leakage paths by MMR survey, shows a thick permeable fractured band of a fault, while other samples from BH-4, BH-5, and BH-7 shows relatively good condition of jointed rock mass (Figs. 25-27). Some minor fractured zones show up in logs for BH-4, BH-5, and BH-7 (Figure 27), but not any dominating ones. According to the MMR survey, the center elevation of the primary and secondary leakage path is expected to be near EL.192 m (GL. -18.9 m) and EL.195m (GL. -22 m) underneath the seepage collection wall. According to the borehole drilling and sampling (Figure 25), BH-1 clearly shows a permeable geologic weakness zone (a fault fracture band) at EL. 194.9 m ~ 185.8 m (GL. -16 ~ -25 m), which is in very good agreement with the predicted primary leakage path of the MMR survey result. The specimen within the fault fracture in BH-1 and BH-2 were easily broken into pieces when pressed by hands. Also, BH-3 (which is predicted as the secondary leakage path) sampling core shows a highly-fractured band as noted in Figure 26. BH-3 shows core loss or rock fracture zone at EL. 202.0 m ~ EL. 194.0 m (GL. -15 m ~ -23 m), which is comparable to the secondary leakage path predicted by the MMR survey. For BH-6, which is relatively closer to predicted primary leakage path, fractured zone also appears in the depth of 29.5 to 33 m. Note that upper 11~12 m thick layer is composed of granular fill material, not the original foundation rock mass.

Overall, it is well validated that the new MMR survey can effectively map the 3D underground preferential flow paths generated by geologic weak layers such as fault fracture band.

According to the YD dam construction records, it is stated that the 20 m width of the fault line is distributed in the center of the dam, with the strike of N5~10W and the dip direction of 75~85NE perpendicular to the plinth axis. In other words, there is a fault zone passing through the dam body and the seepage collection wall. From the results of borehole drilling and seismic tomography, it was confirmed that there is a fault fracture zone on the main leakage path of the MMR survey. The distribution of the fault zone generally agrees with that of YD dam construction records.

Table 2 : Summary of borehole drilling results

Borehole	**Strata**	**Depth range**		**Thickness (m)**	**TCR/RQD (%)**
		GL. -m	**EL. m**		
BH-1	Fill	0.0~11.8	210.87~199.07	11.8	
		11.8~13.5	199.07~197.37	1.7	-
		13.5~16.0	197.37~194.87	2.5	-
	Bedrock	16.0~25.0	194.87~185.87	9.0	27~57 / 0~37
		25.0~31.0	185.87~179.87	6.0	100 / 93
BH-2	Fill	0.0~9.7	210.49~200.79	9.7	
	Weathered rock	9.7~13.0	200.79~197.49	3.3	50 / 5
	Bedrock	13.0~31.0	197.49~179.49	18.0	3~56 / 0~50
		31.0~34.0	179.49~176.49	3.0	90 / 50

BH-3	Fill	0.0~13.0	217.06~204.06	13.0	
	Weathered rock	13.0~15.0	204.06~202.06	2.0	-
	Bedrock	15.0~18.0	202.06~199.06	3.0	30~70 / 0
		18.0~25.0	199.06~192.06	7.0	90~100 / 23~75
BH-4	Fill	0.0~11.9	211.02~198.52	11.9	
	Weathered rock	11.9~12.5	198.52~198.02	1.1	50 / 8
	Bedrock	12.5~15.0	198.02~196.02	2.5	80~98 / 20~30
BH-5	Fill	0.0~9.5	210.44~200.94	9.5	
	Bedrock	9.5~11.3	200.94~199.14	1.8	98 / 15
BH-6	Fill	0.0~11.5	210.86~199.36	11.5	
		11.5~12.0	199.36~198.86	0.5	-
	Bedrock	12.0~29.5	198.86~181.36	17.5	93~100 / 0~40
		29.5~31.4	181.36~179.46	0.9	17~88 / 0~7
		31.4~34.0	179.46~176.87	2.4	
BH-7	Fill	0.0~12.0	210.72~198.72	12.0	
	Bedrock	12.0~34.0	198.72~176.72	22.0	65~97 / 0~39

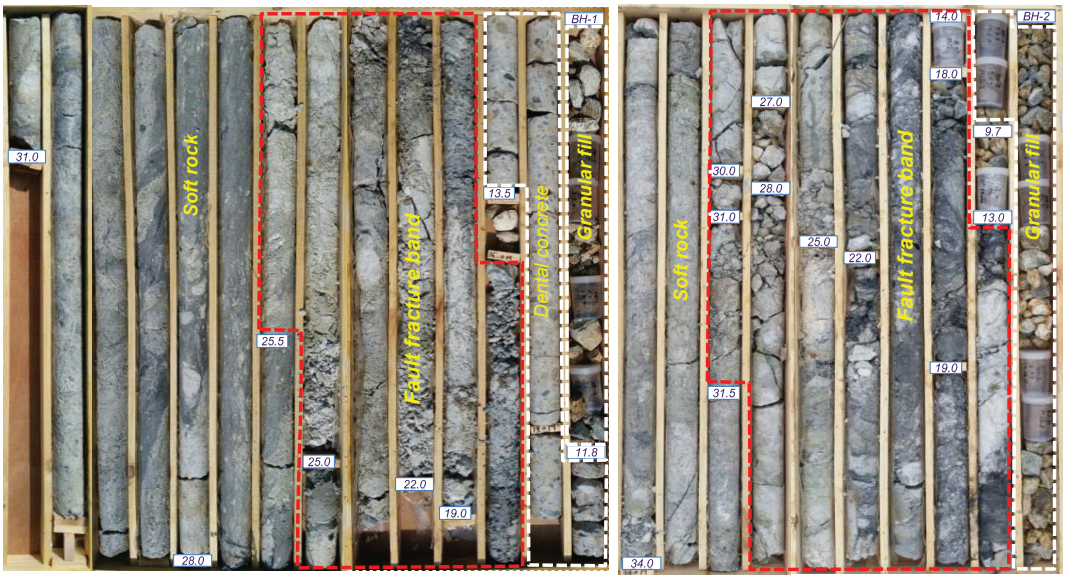

(a) BH-1 (b) BH-2

Figure 25 : BH-1 and BH-2 sampling cores

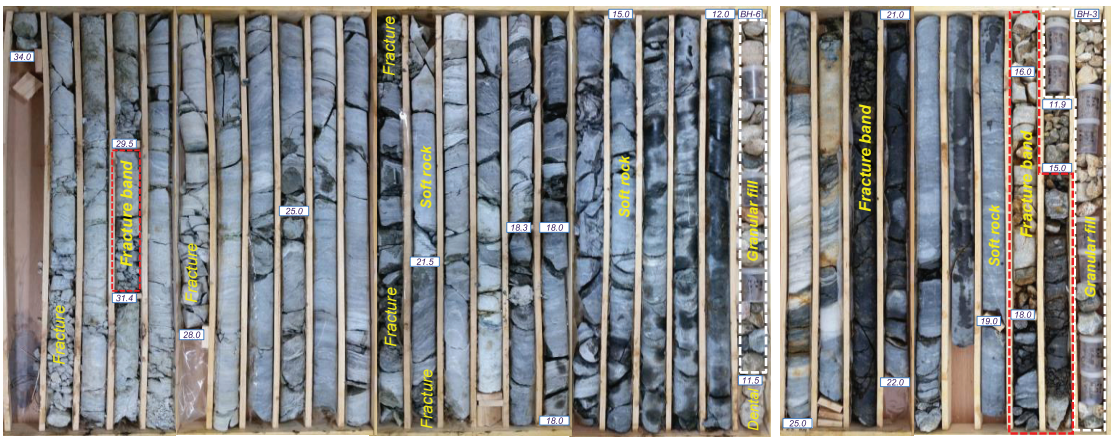

(a) BH-6 (b) BH-3

Figure 26 : BH-6 and BH-3 sampling cores

Figure 27 : BH-5, BH-4, and BH-7 sampling cores

The result of the seismic tomography is shown in Figure 28. The seismic velocity was highest in the upper soft rocks of BH-6. The dental concrete part of BH-6 and BH-1 also showed relatively high velocity. The low velocity band is somewhat widespread in the lower part of BH-6, in the fault zone of BH-1, and in the lower prat of BH-7. The location of fault fracture bands in BH-1 and BH-6 are in good agreement with the result of the seismic tomography.

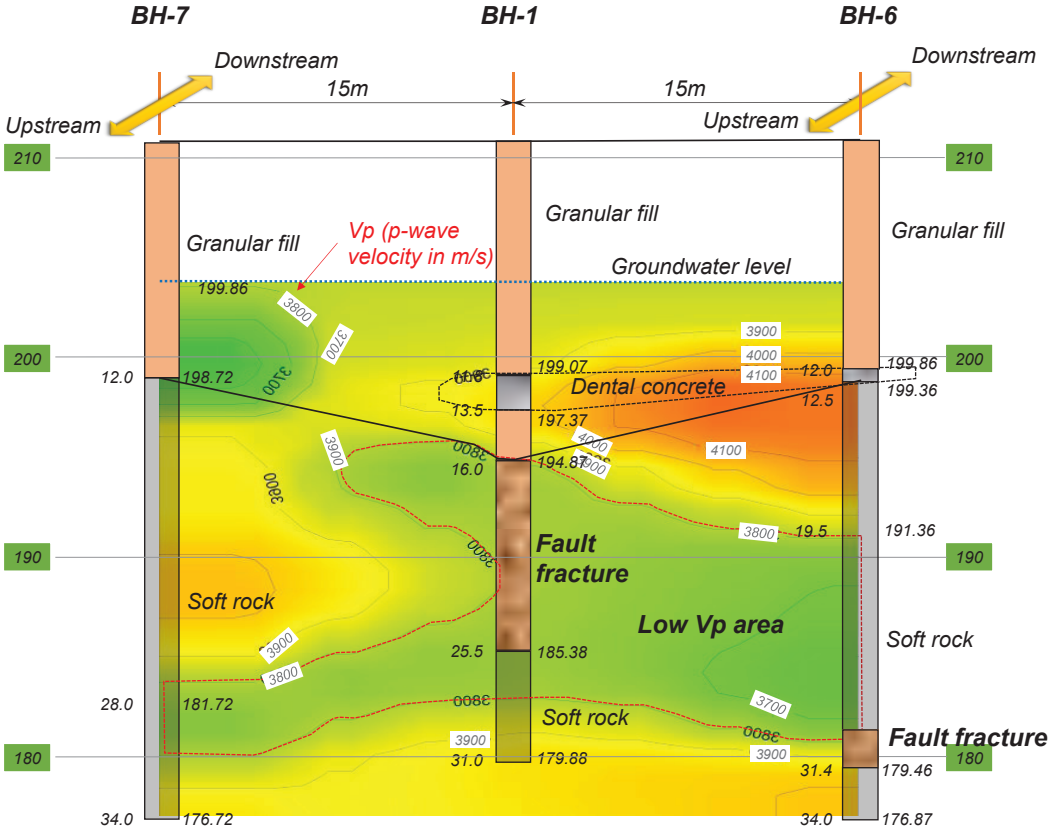

Figure 28 : Seismic tomography results

As a result of Lugeon test, the computed permeability coefficient (k) was 2.01 × 10^{-3} ~ 6.26 × 10^{-4} cm/sec for the fractured rock mass (Table 3). The permeability coefficient of the geologic weakness zone in this study is considered to be the range which enables dissipation of water by steady leakage, which is consistent with the results of borehole drilling and sampling. In particular, the Lugeon value (Lu) of fractured rock mass in BH-2 was 27, which is highly permeable. The flow type of Lugeon test in fractured rock of BH-2 was classified as turbulent flow. This turbulence is generally a flow that occurs in rocks where the discontinuity is partially open or has a medium discontinuity spacing (Houlsby 1976, Lancaster-Jones 1975). From these test results, it is believed that the discontinuity of the fault fracture zone was somewhat open during loading.

Table 3 : Lugeon test result

Borehole	Depth (GL.-m)	Strata	Permeability coefficient (cm/sec)	Lugeon	Remarks
BH-2	23.0~28.0	Fault fracture	3.70×10^{-4}	27	Turbulent flow
	29.0~34.0	Fault fracture ~ soft rock	2.01×10^{-4}	0.6	Dilation
BH-3	16.0~21.0	Soft to hard rock	6.26×10^{-4}	19	Dilation Test stopped by packer breakage

The results of the flow orientation and velocity test are shown in Figure 29 with borehole location and MMR survey result. The meaningful result was obtained from flow orientation at BH-1 that the both flow directions within the fault fracture band is in good agreement of the direction of the predicted primary leakage path. However, since the orientations of BH-1 and BH-2 show very different directions, it is impossible to grasp the connectivity between two points. Part of the reason for this would be that the groundwater flow of rocks with joints and fractures can be greatly affected by the local discontinuity orientation and joint direction.

The calculated flow velocity was 3.5 ~ 5.5 * 10^{-4} cm/s for the geologic weakness zone of boreholes. The result is in good agreement with the Lugeon test result. MMR survey to map preferential flow paths from geologic weakness zone was confirmed by the permeability coefficient as well as seismic tomography and borehole sampling observation.

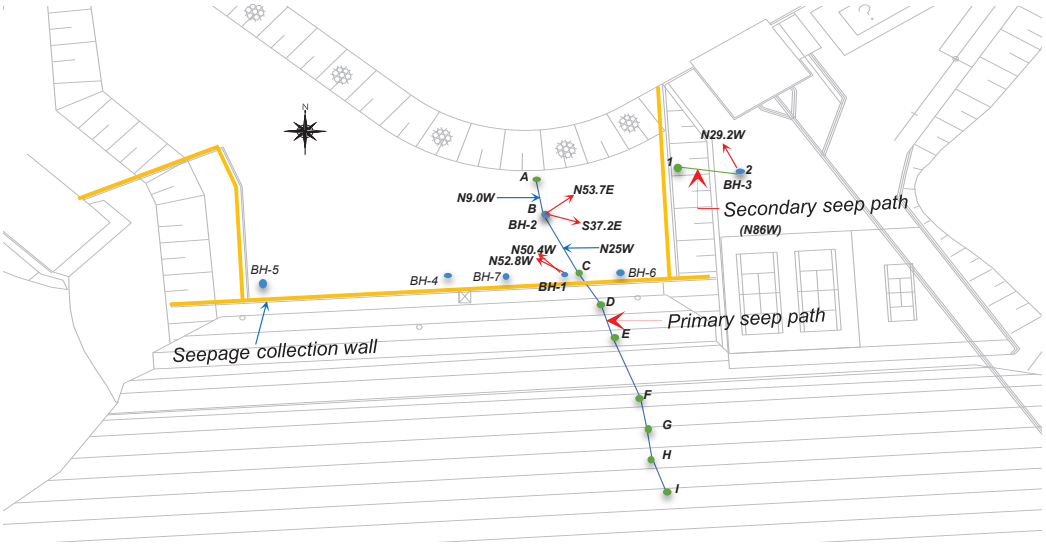

Figure 29 : Distribution of planar distribution in the direction of groundwater

6. DISCUSSION

The Willowstick MMR method is an imaging technology designed for mapping groundwater. It is different from DC Resistivity technologies such as Electrical Resistivity Tomography (ERT), High Resolution Resistivity, and Electrical Resistivity Imaging (ERI).

The DC resistivity method energizes the subsurface from various standpoints to measure the apparent resistivity of the bulk material. The voltage or potential difference between electrodes at the earth's surface is measured (receiver) to calculate the apparent resistivity for each source/receiver setup when electrical current spreads out from the source into the subsurface volume. Resistivity is the inverse of conductivity, so low resistivity indicates high conductivity.

Resistivity sounding and profiling can yield pseudo-sections of the subsurface, not true cross-sections due to the inaccuracy of the underlying assumption that the subsurface is homogeneous or horizontally layered. Surveying multiple parallel and/or perpendicular lines allows 3D information to be gathered. With 3D data, subsurface structures can be delineated better in both horizontal and vertical extent. The value of the DC resistivity method is its ability to delineate geologic structure boundaries that have contrasting resistivities to their surroundings.

The (Willowstick) MMR survey, on the other hand, directly energizes the water of interest with an alternating current (AC). As with all electrical circuits, electric current will choose the paths of least resistance between strategically placed electrodes. The MMR survey is principally used to map concentrated groundwater flow paths where the start and end are known such as leaks in dams, weaknesses in barriers and water flow through high porosity zones (faults, fractures and karst features). These features represent the paths of least resistance to electric current flow between the strategically placed electrodes.

The MMR survey's principal measurement is the magnetic field, not the electric field. The magnetic field is generated by non-inductive electrical current flowing through a conductive path (Biot-Savart Law). The magnetic field has the same frequency as the injected electrical current, so the signal can be distinguished from other noise sources like the power grid (50 or 60 Hz) and its harmonics. Measuring the magnetic field (pure magnetic field not MMR field) has several advantages:

- The magnetic field is directly related to electric current flow; therefore, modeling electric current flow is a simple and direct application of established physical principles (Biot-Savart Law).
- The magnetic field is not shielded by overlying conductive layers such as shale and clay.
- The magnetic field can be measured easily and rapidly with proper equipment, without requiring galvanic contact with the ground.

Both DC resistivity and the MMR survey have their appropriate applications and can be used to complement each other in characterizing the subsurface. Although the MMR survey identifies zones of preferential seepage flow, it does not directly identify the volume of water or the groundwater flow direction. While direction of flow can be safely assumed when elevations are known, seepage flow rates should be determined by other field methods.

7. CONCLUSTION

Identifying underground leakage paths is highly important for the safety reasons owing to seepage in hydraulic structures. However, in the past there have been few techniques to map underground preferential flow paths reliably.

In this study, a newly developed Willowstick MMR survey was introduced in the testbed dam site (YD dam) for the mapping of the underground leakage paths. YD dam had an issue that the seepage rate at the downstream toe was not measured since the end of construction because of potential leakage through or underneath the downstream seepage collection wall. As the signature electric current flows between strategically placed electrodes (located upstream and downstream of the wall), it concentrates in the more conductive zones (i.e., in areas of highest transport porosity) where water preferentially bypasses the wall. The magnetic field signature of the electric current is then measured and modeled to identify patterns of preferential flow that are interpreted to characterize how and where seepage occurs.

Application of the MMR survey to YD dam shows that the MMR survey identified primary and secondary leakage paths through the bottom part of the collecting water retaining wall and provided centerline coordinates of the 3D flow paths. As a result of the geotechnical investigation for the validation, borehole sampling close to the expected flow paths showed the geologic weakness fracture bands of foundation rock-mass. According to the Lugeon test, flow orientation and velocity test, the fracture bands are working as a seepage dissipation passages with permeability coefficient of 10-4 cm/s. The locations and approximate depths of geologic weakness are in good agreement with the MMR survey result. The (Willowstick) MMR survey was able to characterize the underground flow paths effectively.

The 3D resistivity survey was effective in detecting groundwater level, but limited as it pertains to in mapping the geologic weak zone or leakage paths.

Since the existing technology to reliably map the underground leakage is very limited, the newly developed MMR survey is believed to be useful to solve seepage-related problems of hydraulic structures. Contrary to the existing electric field measurement, the technology measures the magnetic field after directly energizing the water of interest, which is beneficial to enhance reliability in that the magnetic field is not shielded by overlying conductive layers and modeling result directly represents a conductive flow path.

The results of the investigation will help make informative decisions concerning how to further identify, monitor and/or possibly remediate seepage out from beneath the seepage collection wall.

ACKNOWLEDGEMENT

The manuscript was prepared for the conference in an expanded version of Park & Jessop (2018). The study was conducted as part of the K-water Research Institute project (2014.01-2016.12), "A study on the integrity assessment of aging dams for dam performance improvement".

REFERENCES

Bruggemann, D.A. & Francis, O.J. 2014. Remedial grouting at Shon Sheffrey dam, Wales, Maintaining the Safety of our Dams and Reservoirs: *Proceedings of the 18th Biennial Conference of the British Dam Society at Queen's University, Belfast, from 3–6 September 2014*. 125-134, ICE Publishing.

Charles, J. 2001. Internal erosion in European embankment dams. *ICOLD European Symposium*, Geiranger, Norway.

Cho, I.-K. & Yeom, J.-Y. 2007. Crossline resistivity tomography for the delineation of anomalous seepage pathways in an embankment dam. *Geophysics* 72: G31-G38.

Edwards, R.N. & Nabighian, M.N. 1991. The magnetometric resistivity method. *Electromagnetic methods in applied geophysics: Investigations in Geophysics 2*. 47-104.

Fell, R., MacGregor, P., Stapledon, D., Bell, G. & Foster, M. 2015. *Geotechnical engineering of dams*, 2nd edition ed. CRC Press Taylor & Francis Group, London, UK.

Fell, R., Wan, C.F., Cyganiewicz, J. & Foster, M. 2003. Time for development of internal erosion and piping in embankment dams. *Journal of Geotechnical and Geoenvironmental Engineering* 129: 307-314.

FEMA. 2015. *Evaluation and monitoring of seepage and internal erosion*. Federal Emergency Management Agency.

Houlsby, A. 1976. Routine interpretation of the Lugeon water-test. *Quarterly Journal of Engineering Geology and Hydrogeology* 9: 303-313.

ICOLD. 1987. *Dam safety guidelines*. International Commission on Large Dams.

ICOLD. 1994. *Aging of dams and appurtenant works - Review and recommendations*. International Commission on Large Dams.

ICOLD. 1995. *Dam failures - Statistical analysis*. International Commission on Large Dams.

ICOLD. 2000. *Rehabilitation of dams and appurtenant works - state of the art and case histories*. International Commission on Large Dams.

ICOLD. 2013. *Internal erosion of existing dams, levees and dikes, and their foundations*. International Commission on Large Dams.

Johansson, S. & Dahlin, T. 1996. Seepage monitoring in an earth embankment dam by repeated resistivity measurements. *European Journal of Engineering and Geophysics* 1: 229-247.

K-water Research Institute. 2016. *A study on the integrity assessment of aging dams for dam performance improvement (III)*. K-water (Korea Water Resources Corporation), Daejeon.

KNCOLD. 2004. *Dams in Korea*. Korea National Committee on Large Dams.

Kofoed, V.O., Montgomery, J.R., Jeffery, R.N., Montgomery, N.R., Jessop, M.L., Wallace, M.J. & Christensen, B.A. 2013. *System for detecting a location of a subsurface channel*. U.S. Patent Application No. 13/778,463.

Kofoed, V., Montgomery, J. & Gardiner, K. 2006. Identifying leakage paths in earthen embankments, Improvements in reservoir construction, operation and maintenance: *Proceedings of the 14th Conference of the British Dam Society at the University of Durham from 6 to 9 September 2006*. 119-128, Thomas Telford Publishing.

Kofoed, V.O., Jessop, M.L. & Wallace, M.J. 2012. Assessing seepage flow conditions through a dam quickly and accurately without drilling or drawing down the reservoir. *25th Symposium on the Application of Geophpysics to Engineering & Environmental Problems*.

Lancaster-Jones, P. 1975. The interpretation of the Lugeon water-test. *Quarterly Journal of Engineering Geology and Hydrogeology* 8: 151-154.

Lim, H.D., Lee, K.H., Lee, J.Y. & Oh, B.H. 2004. Leakage investigation, remedial works and its effects on seepage control of Unmun dam. *ICOLD 72nd Annual Meeting, Proceedings Workshop on Dam Safety Problems and Solutions—Sharing Experience*, KNCOLD (CD-Rom), 225-243.

Montgomery, J. & Kofoed, V.O. 2008. Characterizing groundwater using controlled source audio frequency domain magnetics. *Symposium on the Application of Geophysics to Engineering and Environmental Problems 2008*. Society of Exploration Geophysicists, 969-972.

Nolet, G. 1987. Seismic wave propagation and seismic tomography. *Seismic tomography*. Springer, 1-23.

Panthulu, T., Krishnaiah, C. & Shirke, J. 2001. Detection of seepage paths in earth dams using self-potential and electrical resistivity methods. *Engineering Geology* 59: 281-295.

Park, D.S. & Jessop, M.L. 2018. Validation of a new magnetometric survey for mapping 3D subsurface leakage paths. *Geosciences Journal*. 22(6): 891-902.

Park, D.S. & Oh, J.H., 2016. Potential hazard classification of aged cored fill dams. *The Korean Journal of Engineering Geology* 26: 207-221.

Purvance, D.T. & Andricevic, R. 2000. On the electrical-hydraulic conductivity correlation in aquifers. *Water Resources Research* 36: 2905-2913.

Rice, J.D. & Duncan, J.M. 2009. Findings of case histories on the long-term performance of seepage barriers in dams. *Journal of Geotechnical and Geoenvironmental Engineering* 136: 2-15.

Samouëlian, A., Cousin, I., Tabbagh, A., Bruand, A. & Richard, G. 2005. Electrical resistivity survey in soil science: a review. *Soil and Tillage research* 83: 173-193.

Sjödahl, P., Dahlin, T., Johansson, S. & Loke, M. 2008. Resistivity monitoring for leakage and internal erosion detection at Hällby embankment dam. *Journal of Applied Geophysics* 65: 155-164.

Smith, M., Côté, A., Noël, P. & Babin, D. 2009. Characterizing seepage at the junction of two embankment dams. *Annual Conference of the Canadian Dam Association*.

U.S. Army Corps of Engineers. 1993. *Seepage analysis and control for dams*. U.S. Army Corps of Engineers, Washington, DC.

Wilkinson, P., Meldrum, P., Kuras, O., Chambers, J., Holyoake, S. & Ogilvy, R. 2010. High-resolution electrical resistivity tomography monitoring of a tracer test in a confined aquifer. *Journal of Applied Geophysics*. 70: 268-276.

Yaramanci, U., Kemna, A. & Vereecken, H. 2005. Emerging technologies in hydrogeophysics. *Hydrogeophysics*. Springer, 467-486.